nature chemistry

ARTICLES

PUBLISHED ONLINE: 13 APRIL 2014 | DOI: 10.1038/NCHEM.1918

Templated assembly of photoswitches significantly increases the energy-storage capacity of solar thermal fuels

Timothy J. Kucharski[1,2]*, Nicola Ferralis[1], Alexie M. Kolpak[3], Jennie O. Zheng[1], Daniel G. Nocera[2]* and Jeffrey C. Grossman[1]*

Large-scale utilization of solar-energy resources will require considerable advances in energy-storage technologies to meet ever-increasing global energy demands. Other than liquid fuels, existing energy-storage materials do not provide the requisite combination of high energy density, high stability, easy handling, transportability and low cost. New hybrid solar thermal fuels, composed of photoswitchable molecules on rigid, low-mass nanostructures, transcend the physical limitations of molecular solar thermal fuels by introducing local sterically constrained environments in which interactions between chromophores can be tuned. We demonstrate this principle of a hybrid solar thermal fuel using azobenzene-functionalized carbon nanotubes. We show that, on composite bundling, the amount of energy stored per azobenzene more than doubles from 58 to 120 kJ mol^{-1}, and the material also maintains robust cyclability and stability. Our results demonstrate that solar thermal fuels composed of molecule–nanostructure hybrids can exhibit significantly enhanced energy-storage capabilities through the generation of template-enforced steric strain.

Solar-energy utilization necessitates a storage method because of its local intermittency and the daily and seasonal temporal mismatch between supply and demand. Two major approaches for storing solar energy are electrochemical storage following conversion into a photocurrent and photoelectrochemical generation of combustible fuels[1]. Although the former is convenient because the storage materials are cyclable, achieving further increases in energy densities and improving transportability both remain significant challenges to large-scale electrochemical energy storage[2,3]. Combustible fuels are the most widely used source of stored energy, and they are transported readily in a high energy-density form as liquids. Although solar water-splitting to give fuels is advancing with the likes of an artificial leaf[4,5], the efficient storage of solar energy in liquid fuels on non-geological timescales continues as an unanswered challenge[6]. Furthermore, the success of this approach would still require the development of solutions to the issue of CO_2 emissions[7].

For applications in which heat is desired[8], an additional method for storing solar energy is the use of solar thermal fuels, which combine the advantages of emission-free cyclability and transportation potentially in a high energy-density form. In contrast to traditional combustible fuels, solar thermal fuels operate in a closed cycle. On light absorption ($E_{h\nu}$), fuel molecules in the ground state undergo photoisomerization into a metastable state, storing enthalpy ΔH (the difference in enthalpy between the two isomers). Later, the stored energy can be released as heat by triggering the reverse thermal isomerization process[9]. The molecules are converted back into the stable isomer in this process, which makes solar thermal fuels inherently emission-free, renewable on useful timescales and renewable locally and off-grid because only sunlight is needed for regeneration.

The criteria that must be met for a practical solar thermal fuel are discussed elsewhere[9–13], but essentially they are a large ratio of $\Delta H/E_{h\nu}$, an absorbance spectrum that overlaps well with the solar spectral irradiance, a high and uniform efficiency of light absorption, a high quantum yield for photoisomerization to the metastable isomer and a non-absorbing metastable isomer (that is, the molecule is strongly photochromic). Perhaps the most challenging criterion to achieve for solar thermal fuels is a large energy density (ΔH) because structural isomerization generally requires (releases) 2–4 orders of magnitude less energy than the breaking and forming of chemical bonds during the combustion of common liquid fuels[9]. The absence of a demonstration of a pathway to increasing ΔH in photochromic pairs for use as solar thermal fuels (despite a great deal of work, for example on norbornadiene/quadricyclane[10,14] and various organometallics[15–18]) is clear evidence of the significant challenges for molecular and materials design.

Here we demonstrate our approach for increasing ΔH by templating photoswitches on nanostructures, which move beyond a discrete molecular regime, and thereby enable a vastly expanded parameter space for the design of new solar thermal materials. The novelty of this approach is embodied in the decoupling of molecular properties to allow for the tuning of thermodynamic (ΔH) and kinetic (storage lifetimes) parameters while only minimally perturbing photochemical parameters and maintaining robust cyclability. This work represents the first proof-of-principle for increasing ΔH and the thermal stability of a photochromic pair of isomers through templating alone.

Results and discussion

Selection of the chromophore–template pair. The major challenge for realizing a templating approach for solar thermal fuels is the covalent functionalization of locally rigid, low-mass nanostructures at high-enough functionalization densities to both enforce and take advantage of highly strained molecular

[1]Department of Materials Science and Engineering, Massachusetts Institute of Technology, Cambridge, Massachusetts 02139, USA, [2]Department of Chemistry and Chemical Biology, Harvard University, Cambridge, Massachusetts 02138, USA, [3]Department of Mechanical Engineering, Massachusetts Institute of Technology, Cambridge, Massachusetts 02139, USA. *e-mail: tkuch@mit.edu; dnocera@fas.harvard.edu; jcg@mit.edu

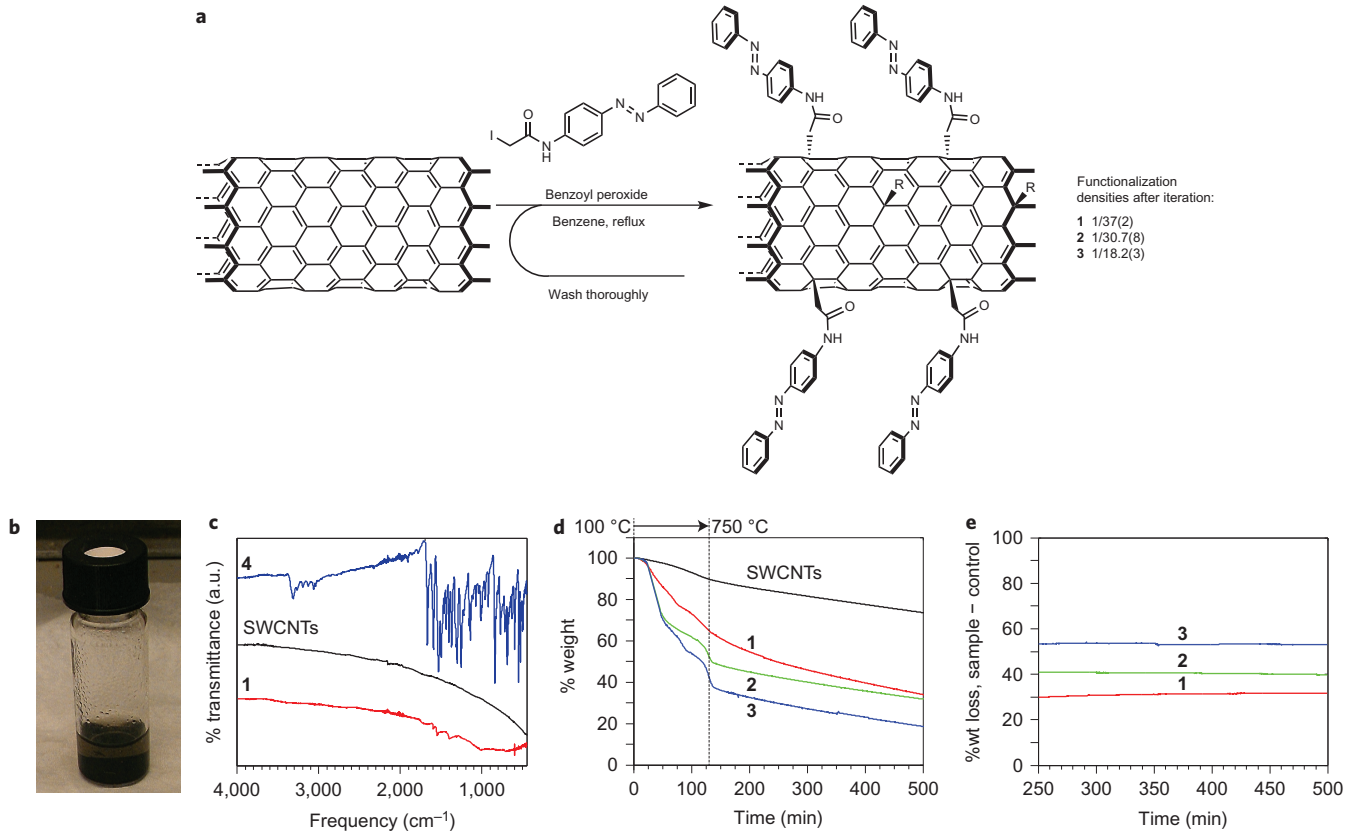

Figure 1 | Synthesis and characterization of azobenzene-functionalized SWCNTs. a, Synthetic scheme for the iterative functionalization of SWCNTs with azobenzenes. **b**, A suspension of SWCNTs functionalized with ethyl 4-butylate in acetone after standing undisturbed for one month. **c**, FTIR spectra of free azobenzene Azo-**4**, pristine SWCNTs and Azo-SWCNT **1**. **d**, Representative TGA plots of pristine SWCNTs and Azo-SWCNTs **1**, **2** and **3** heated from 100 to 750 °C and held at 750 °C, which yielded a constant degradation rate with respect to time once the functional groups were removed. **e**, The difference in mass loss between samples of Azo-SWCNTs **1**, **2** and **3** and pristine SWCNTs during the constant-rate decomposition of SWCNTs, which yielded averages of 31.2(5), 40.4(3) and 53.3(2) wt% functional groups for Azo-SWCNTs **1**, **2** and **3**, respectively (see Supplementary Information for the full data set). a.u., arbitrary units.

configurations generated photochemically. One of the most promising candidate chromophore/template systems indicated by our computational screening was azobenzene-functionalized single-walled carbon nanotubes (SWCNTs) with a functionalization density of one azobenzene chromophore for every eight SWCNT carbon atoms (noted as 1/8)[19,20]. Although using a light-absorbing template such as a SWCNT is not ideal, this type of disadvantage is minimized at high functionalization densities by minimizing the mass fraction of the template and by disrupting the conjugation that leads to the electronic transitions responsible for absorption.

Our prior computational modelling showed that even without engineering inter- and intramolecular hydrogen bonding, close packing via templating increased the amount of energy stored per azobenzene by 30% versus that of the free analogue[19]. To observe any of these effects, the intermolecular packing must approach, at least locally, a level corresponding to that of a (2*n*,0)-SWCNT with a functionalization density of 1/8 (that is, ~4.24 Å separation down the long axis of the SWCNT), and the azobenzenes must be bound covalently to prevent undesired relaxation of the (con)strained systems once generated. Thus, we set out to test azobenzene-functionalized SWCNTs (Azo-SWCNTs) as an initial proof-of-principle for our new approach to molecular hybrid nanostructures for solar thermal fuels, focusing on the effect of template-enforced steric restriction. As discussed below, we synthesized Azo-SWCNTs with a functionalization density of 1/18.2(3). Along with a non-templated molecular analogue, these Azo-SWCNTs allowed us to probe the effect of packing as a result of templating under different conditions: in dilute suspensions there are minimal packing interactions, whereas the solid-state bundling of the Azo-SWCNTs can increase the effective functionalization density (decrease the intermolecular separation) by roughly twofold, which leads to the desired packing interactions (as discussed later and depicted in Fig. 4).

Synthesis of azobenzene-functionalized SWCNTs. There are few methods that covalently functionalize SWCNTs[21,22] to the extent required for our purposes. Prior to this work, multi- and single-walled carbon nanotubes had been modified with azobenzenes[23] only non-covalently or covalently at functionalization densities orders of magnitude lower than those needed to observe attractive solar thermal energy density and storage-lifetime properties. As a starting point for our synthetic method, we chose to append the linkers to the SWCNTs via organic radicals, a method that had been demonstrated previously to yield functionalization densities as high as 1/5 for simple alkyl fragments[24]. We tested two approaches to the synthesis of Azo-SWCNTs: (1) appending a high density of linkers that contain esters for subsequent conversion into azobenzene amides (Supplementary Fig. 1), and (2) direct functionalization with organic radicals with amide-linked azobenzenes, as shown in Fig. 1a.

Initial functionalization of SWCNTs via route (1) yielded a functionalization density of 1/19 in a single step as determined by thermogravimetric analysis (TGA; details in the Supplementary Information) after repeated resuspension and washing to remove any molecules not covalently bound to the SWCNTs. However,

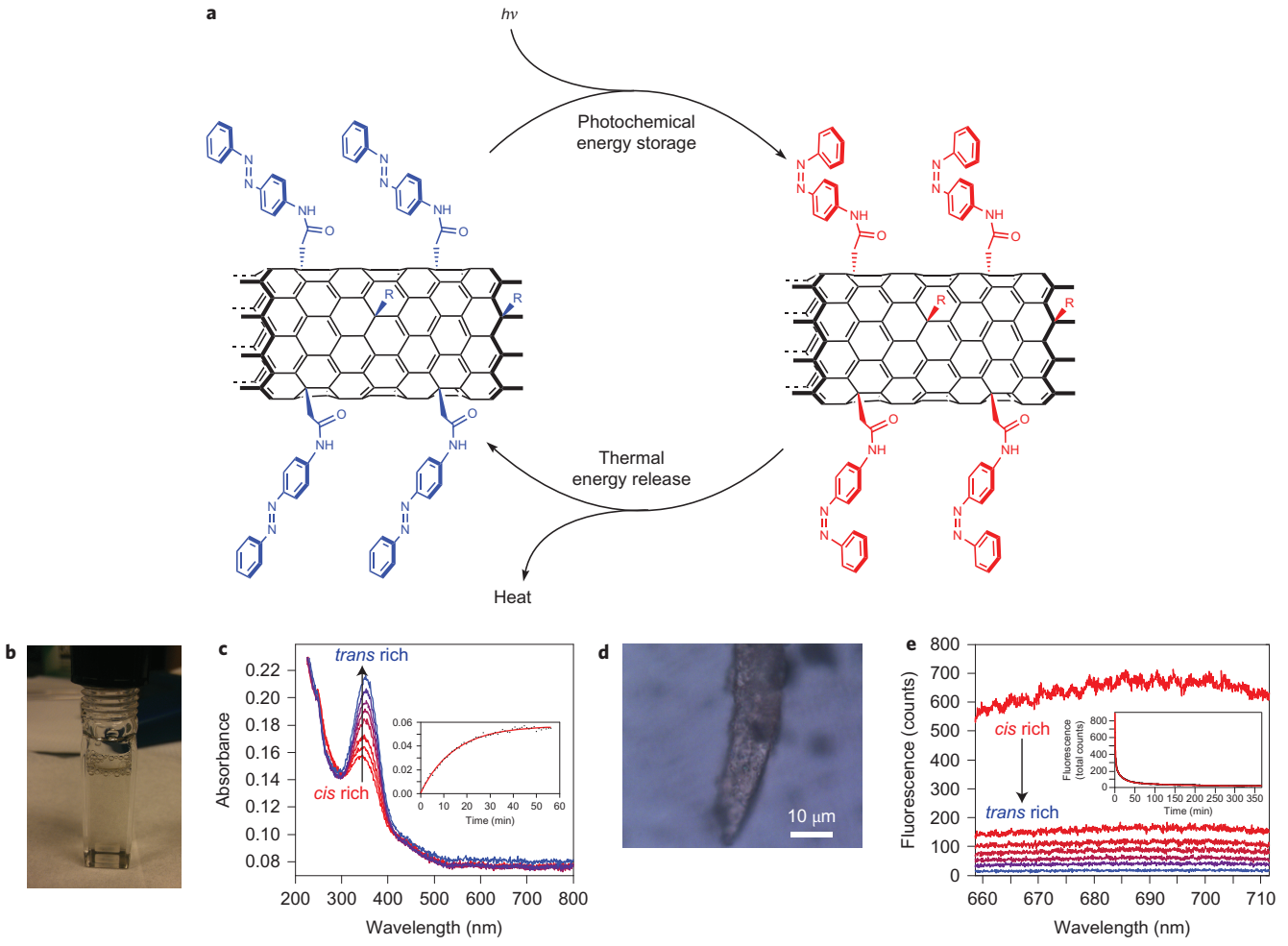

Figure 2 | Photochemical charging and thermal energy release. a, Reaction scheme for photochemical charging and thermal activation of energy release in Azo-SWCNTs. **b**, A dilute suspension (120 mg l^{-1}) of Azo-SWCNT **3** in acetonitrile for thermal isomerization kinetics measurements. **c**, Time-resolved ultraviolet–visible spectra indicate the thermal *cis* → *trans* isomerization in the sample shown in **b** heated to 75 °C. The inset shows the monoexponential increase in absorbance at 350 nm over time. **d**, Optical micrograph of a bundle of Azo-SWCNT **3** drop-cast and dried on a glass slide. **e**, Time-resolved fluorescence spectra indicate thermal *cis* → *trans* isomerization in the sample shown in **d** with the stage heated to 80 °C. The inset shows the change in total counts over time, which does not exhibit monoexponential kinetics.

subsequent chemical modification of such ester-functionalized SWCNTs led either to an overall loss of functional groups or to the presence of an undesirable mixture of functional groups. The drawback to the direct functionalization approach (route (2)) is the limited solubility of the azobenzene-containing precursor in the reaction medium at the levels of excess needed to drive the process in a single step to high functionalization densities with bulkier groups. However, we found that iterating the radical-initiated functionalization process resulted in a steady increase in functionalization densities, as seen with the longer ethyl 4-butanoate (pristine → 1/93(2) → 1/46(3) → 1/21(2), Supplementary Fig. 2) and *N*-(4-azobenzene)acetamide (pristine → 1/37(2) → 1/30.7(8) → 1/18.2(3), denoted as Azo-SWCNT **1**, **2** and **3** (Fig. 1a; details regarding SWCNT diameters and defect densities are given in the Supplementary Information). Once functionalized, Azo- and ester-SWCNTs can be suspended indefinitely in in polar organic solvents such as acetonitrile and acetone (Fig. 1b).

Characterization, photoisomerization and thermal isomerization kinetics. The presence of azobenzenes bound to the SWCNTs is supported by the observation of new bands in the Fourier transform infrared (FTIR) spectra of Azo-SWCNT **1** (Fig. 1c) that can be assigned to the C=O stretch (broad 1,676 cm^{-1}), the N–H bend (1,595 cm^{-1}) and the N=N stretch (1,394 cm^{-1}) by comparison to those of the model compound 4-acetamidoazobenzene (Azo-**4**; 1,669, 1,594 and 1,405 cm^{-1}, respectively) and frequencies calculated by density functional theory (DFT; details given in the Supplementary Information). The increase in bulk-average functionalization density was determined by the corresponding increase in fractional mass loss on heating to 750 °C (Fig. 1d,e).

At sufficiently high functionalization densities (Azo-SWCNT **3**), an absorbance band at ~350 nm, attributable to the $\pi \rightarrow \pi^{\star}$ transition of the appended azobenzenes, appears in the optical absorbance spectra of dilute acetonitrile suspensions. Irradiation of dilute suspensions (120 mg l^{-1}) of Azo-SWCNT **3** at 350 nm generated a photostationary state consisting of 74% *cis* isomer as determined by fitting the absorption spectra. The similarly prepared photostationary state of the free Azo-**4** consisted of 86±2% *cis* isomer as determined by liquid chromatography–mass spectrometry (details given in the Supplementary Information). The kinetics of the thermal *cis* → *trans* isomerization for Azo-SWCNT **3** and free Azo-**4** in acetonitrile were determined in acetonitrile by irradiating samples at 350 nm followed by heating in the dark at 25–75 °C (Fig. 2a,b). Absorbance versus time at each wavelength over the range 340–360 nm in 1 nm increments

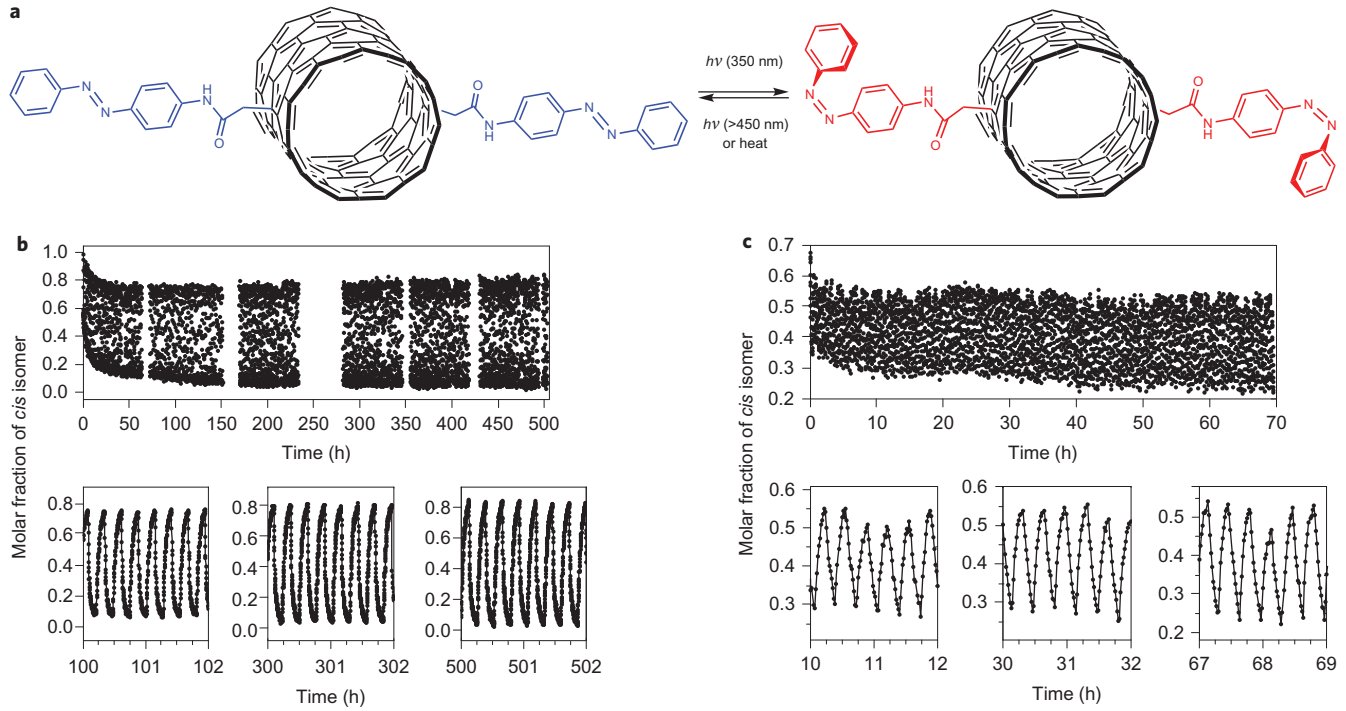

Figure 3 | Photochemical and thermal cycling. a, Reaction scheme for photochemical and photochemical/thermal cycling of Azo-SWCNTs. **b**, Optical cycling of Azo-SWCNT **3** in acetonitrile by alternatively irradiating at 350 and ≥450 nm. Molar fractions are determined by fitting the absorbance spectrum at each time point. The system takes ~60 hours to establish a stable span in molar fraction because each irradiation cycle is not long enough to establish fully a photostationary state. Only every 50th data point is shown in the top plot. Gaps in the data are when the data-recording computer failed, although the irradiation cycles continued uninterrupted. The lower panels show two-hour portions of the data for comparison. **c**, Optical and thermal cycling of Azo-SWCNT **3** in acetonitrile by alternating periods of 350 nm irradiation and dark with the sample held at 75 °C.

exhibited monoexponential kinetics (Fig. 2c) and yielded average first-order rate constants with relative standard errors <0.2% for individual experiments. Activation parameters for the thermal *cis* → *trans* isomerization in a dilute suspension of Azo-SWCNT **3** ($\Delta H^{\ddagger} = 90 \pm 3$ kJ mol^{-1}, $\Delta S^{\ddagger} = -45 \pm 4$ J mol^{-1} K^{-1}, which corresponds to a half-life of ~33 hours at 25 °C) were not statistically different from those of Azo-**4** ($\Delta H^{\ddagger} = 92 \pm 2$ kJ mol^{-1}, $\Delta S^{\ddagger} = -41 \pm 7$ J mol^{-1} K^{-1}) at the 95% confidence level.

By removing the solvent and allowing Azo-SWCNT **3** to bundle in the solid state, we were able to enforce interactions between the azobenzene fragments on neighbouring SWCNTs, which led to regions with average intermolecular separations significantly smaller than those on isolated SWCNTs (further discussion below). In solution, azobenzene is essentially non-fluorescent because of its rapid photoisomerization[25], but it becomes strongly fluorescent when its conformational freedom is restricted by its surroundings and isomerization is inhibited (for example, by aggregation)[26–28]. We observed regions of strong fluorescence in samples of Azo-SWCNT **3** drop-cast and dried on glass (Fig. 2d), which indicates the presence of such conformational restriction, which is not present in dilute suspensions of unbundled Azo-SWCNT **3**. Following ultraviolet irradiation to increase the fraction of *cis* isomers present, solid-state kinetics measurements of the *cis* → *trans* isomerization were carried out under atmospheric conditions by monitoring the decrease in fluorescence yield under monochromatic illumination (Fig. 2e; details in the Supplementary Information). The decrease in fluorescence over time is consistent with the conversion of the more conformationally restricted *cis* isomer to the less-restricted *trans* isomer, and the initial intensity of the fluorescence was reproduced by exposure to ultraviolet radiation to regenerate the *cis* isomers.

These fluorescence measurements revealed that the overall energy-releasing *cis* → *trans* process was no longer monoexponential with respect to time, which suggests the presence of multiple populations of azobenzenes experiencing different local environments, such as those with different bundling and packing densities. Furthermore, measurements with the sample stage heated to 160 °C yielded rate constants 1–5 orders of magnitude slower (half-lives of 1.5 minutes to five hours, assuming the process is a series of concurrent monoexponential processes) than the projected rate constant for thermal *cis* → *trans* isomerization in dilute suspensions of unbundled Azo-SWCNT **3** (projected half-life of one second at this temperature). In some measurements, the kinetic envelope also revealed the presence of non-monotonic events (for example, two small broad features (Supplementary Fig. 15)), which could be an indication of localized time- or temperature-triggered discharging events for areas of particular functionalization or bundle packing density. Future studies will be devoted to the identification of the origin of the diversity of processes at play in such samples.

Cyclability. Suspensions of Azo-SWCNT **3** in acetonitrile continue to exhibit the robust cyclability characteristic of azobenzenes. Irradiating alternatively at 350 and ≥450 nm (Fig. 3a) drives the sample composition towards photostationary states that are more *cis* enriched and *trans* enriched, respectively, than that obtained under broadband irradiation. Optical switching is based on selective irradiation at wavelengths with maximum and minimum values of the ratio of molar absorptivities for the two isomers. Although ideal systems would maintain a high value of this ratio at all wavelengths so that unfiltered solar irradiation yields the greatest amount of charging possible, we were able to repeat this photochemical cycling nearly 2,000 times with no appreciable sign of degradation (Fig. 3b).

Additionally, Azo-SWCNT **3** can be charged with 350 nm irradiation and discharged in the dark at 75 °C for more than 200 cycles without any significant degradation (Fig. 3a,c). Samples of

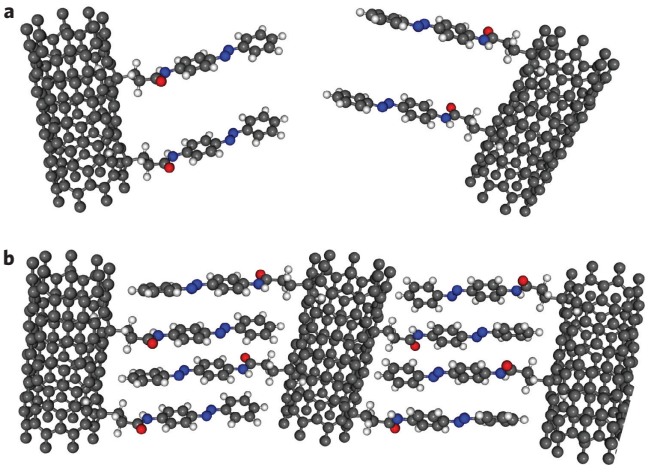

Figure 4 | Effect of packing photochemical switches in the solid state. Illustrations of: **a**, Non-interacting Azo-SWCNTs in a suspension; **b**, interacting Azo-SWCNTs bundled in the solid state.

Azo-SWCNT **3** subjected to such repeated cycling behaved identically to samples not cycled repeatedly, as determined by subsequent thermal isomerization kinetics measurements. Furthermore, solid samples of Azo-SWCNT **3** were subjected to similar repeated charging/discharging cycles. Charging with 350 nm irradiation and thermal discharging at room temperature and atmospheric conditions revealed no degradation, as measured by the reduction and reestablishment of fluorescence yield. No molecular degradation was observed by irradiation with high-density monochromatic illumination (He–Ne laser with a power density $<50\ \mu W\ \mu m^{-2}$).

Energy storage. We determined the enthalpy difference between the *cis* and *trans* isomers, $\Delta H_{cis-trans}$, in Azo-SWCNT **3** and free Azo-**4** using differential scanning calorimetry (DSC). Solid-state samples of Azo-SWCNT **3** obtained from drying *cis*-rich photostationary states prepared in dilute acetonitrile suspensions exhibited a broad exothermic heat flow over 60–130 °C, which corresponds to a bulk gravimetric energy density for the molecule–template composite material of 200 J g^{-1} (56 Wh kg^{-1}). Heat flows from suspensions of Azo-SWCNT **3** at a high-enough dilution to ensure the absence of inter-SWCNT interactions were below the detection limit of our system (see Supplementary Section 9.2 for further discussion). More importantly, however, the exothermic heat flow for (non-templated) molecule Azo-**4** in the solid state occurred over a slightly narrower range (70–125 °C) and corresponded to a bulk energy density of 160 J g^{-1} (44 Wh kg^{-1}).

These DSC results show that the gravimetric energy density of bundled Azo-SWCNT **3** was increased compared to the free analogue, despite the fact that the template made up 48 wt% of the sample. Accounting for the compositions of the photostationary states generated for each sample (details in the Supplementary Information) further indicated that the value of $\Delta H_{cis-trans}$ per azobenzene had more than doubled from 58 kJ mol^{-1} in Azo-**4** to 120 kJ mol^{-1} in bundled Azo-SWCNT **3**. Even under the limiting assumption that all the molecules had been converted into *cis* isomers (thus a minimum amount of energy stored per azobenzene), the energy stored per azobenzene is still a 60% increase (to 92 kJ mol^{-1}) over that of the free analogue Azo-**4**, which is still twice the magnitude of the predicted[19] increase (30%) in $\Delta H_{cis-trans}$ per azobenzene through packing alone.

Potassium ferrioxalate actinometry[29] allowed us to estimate the energy-storage efficiency of bundled Azo-SWCNT **3** as 14% when irradiating at 350 nm (details in the Supplementary Information). The solar-energy storage efficiency under AM1.5 irradiation is estimated to be 0.3%. A detailed derivation of this metric is discussed in the Supplementary Information. For comparison, the solar energy-storage efficiency of triplet-sensitized norbornadiene → quadricyclane (89 kJ mol^{-1}, 970 J g^{-1}, 270 Wh kg^{-1}) is 0.21% and that of photosynthesis is typically 0.1–0.3%[10] .

Intertemplate interactions and the effect of bundling. Our previous work[19] indicates that changes >5 kJ mol^{-1} in the activation barrier for thermal isomerization are observed only at intermolecular separations ($d_{||}$, Fig. 5a) <5 Å. Therefore, the similarity in activation parameters for the thermal *cis* → *trans* isomerization suggests that in dilute suspensions of Azo-SWCNT **3** there are no regions with a local functionalization density much greater than the bulk functionalization density, which would correspond to >8 Å intermolecular separation if homogeneously distributed on (2*n*,0)-SWCNTs. Furthermore, this similarity also indicates that there are negligible intertemplate interactions in such dilute suspensions (Fig. 4a).

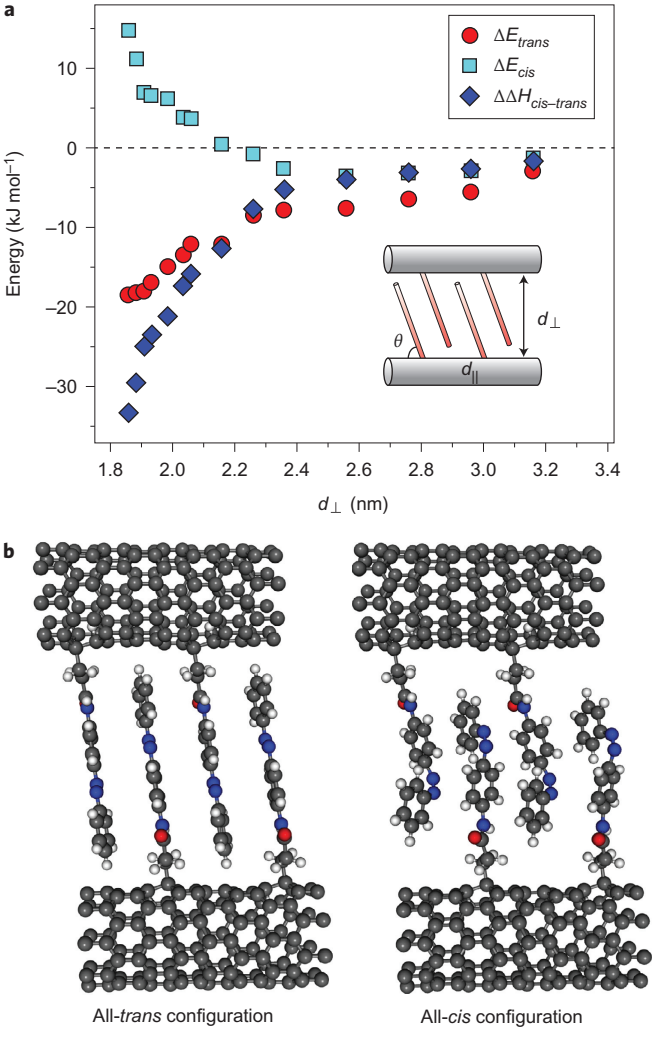

Figure 5 | Energy storage as a function of template-packing parameters. **a**, Enthalpy difference $\Delta H_{cis-trans}$ for intercalated Azo-SWCNTs (blue diamonds), as well as total energy per azobenzene of the *cis* (cyan squares) and *trans* (red circles) conformations, as a function of SWCNT separation. Energies are relative to the respective values for an isolated Azo-SWCNT with 1/16 packing density. The inset schematic defines the geometric parameters. **b**, Computed atomic structures at the minimum-energy *trans* separation distance.

However, when samples of Azo-SWCNT **3** were dried, bundling of the material effectively decreased the intermolecular separations as neighbouring functionalized templates were brought together (Fig. 4b). As discussed above, the presence of strong fluorescence in the solid state is consistent with a conformational restriction of the bound azobenzenes. The decrease in fluorescence yield and subsequent regeneration on exposure to ultraviolet radiation is also consistent with the *cis* isomer being more conformationally restricted than the *trans* isomer. We attribute the observed increase in $\Delta H_{cis-trans}$ to this enhanced difference in strain enforced by the bundled templates. The presence of such conformational restriction is further supported by the inhibition of the thermal isomerization kinetics in the solid state; our original modelling[19] predicted that such steric restriction would effectively increase the activation barrier for the energy-releasing thermal *cis* → *trans* isomerization.

Model refinement. Given the disparity between our earlier prediction[19] of the increase in $\Delta H_{cis-trans}$ from packing alone (30%) and the increase we observed in this work (∼200%), we refined our model to account for configurations with interactions between neighbouring functionalized templates. To do so, we performed DFT calculations (details in the Supplementary Information) for a range of intercalated Azo-SWCNT structures, as shown schematically in Fig. 5a. Assuming a homogeneous functionalization density of 1/16 (similar to the experimental density of ∼1/18, but allowing for a smaller supercell periodicity in the calculations), we determined the minimum-energy configuration of two neighbouring Azo-SWCNTs as a function of the distance between the nanotubes ($d_\perp$) and the angle between the bound azobenzenes and the nanotube axis (θ). When all of the azobenzenes are in the *trans* state, the most favourable structure occurs at $d_\perp \approx 1.86$ nm and $\theta \approx 83^\circ$ (Fig. 5a). In this configuration, the distance between neighbouring nanotubes is similar to the length of the *trans*-azobenzene molecule, which leads to a high effective-packing density of approximately 1/8 parallel to the bundled nanotubes. Computation of the all-*cis* configuration (Fig. 5b) at the same $d_\perp$ (that is, assuming the bundle geometry is determined by the ground-state all-*trans* configuration and does not change significantly on isomerization) gives $\Delta H_{cis-trans} = 92$ kJ mol^{-1}. Furthermore, this value of $\Delta H_{cis-trans}$ and the value for an isolated 1/16 Azo-SWCNT structure ($\Delta H_{cis-trans} = 59$ kJ mol^{-1}) give energy densities of 59 and 38 Wh kg^{-1}, respectively, which bracket the experimental value measured for the bulk gravimetric energy density, as expected given the mixture of different configurations in the solid.

Conclusions

We report a proof-of-principle system that demonstrates our novel approach to achieving solar thermal fuels of high energy density by templating photoswitchable molecules on rigid low-mass nanostructures. We show that the enforcement of conformational restriction and photochemically generated steric strain in chromophore–template constructs can increase both the amount of energy stored per photochromic molecule by more than 200% and the storage lifetimes by orders of magnitude, along with resisting material degradation under repeated cycling. This work establishes the feasibility of increasing bulk gravimetric energy densities of such photochromic molecules despite the obvious potential decrease associated with the addition of a non-energy-storing templating material. Although the composite material reported here, SWCNTs highly functionalized with azobenzenes, does not encompass the inter- and intramolecular hydrogen bonding included in our prior theoretical modelling, our results show that interactions between chromophores on neighbouring templates can potentially be even more important than those on an individual template. This work yet further increases the pool of potential candidate chromophore–template combinations from those previously identified and further emphasizes the importance of enforcing steric strain via templating.

Received 28 December 2013; accepted 6 March 2014; published online 13 April 2014

References

1. Cook, T. R. *et al.* Solar energy supply and storage for the legacy and nonlegacy worlds. *Chem. Rev.* **110,** 6474–6502 (2010).
2. Aricò, A. S., Bruce, P., Scrosati, B., Tarascon, J-M. & van Schalkwijk, W. Nanostructured materials for advanced energy conversion and storage devices. *Nature Mater.* **4,** 366–377 (2005).
3. Dunn, B., Kamath, H. & Tarascon, J-M. Electrical energy storage for the grid: a battery of choices. *Science* **334,** 928–935 (2011).
4. Reece, S. Y. *et al.* Wireless solar water splitting using silicon-based semiconductors and earth-abundant catalysts. *Science* **334,** 645–648 (2011).
5. Nocera, D. G. The artificial leaf. *Acc. Chem. Res.* **45,** 767–776 (2012).
6. Benson, E. E., Kubiak, C. P., Sathrum, A. J. & Smieja, J. M. Electrocatalytic and homogeneous approaches to conversion of CO_2 to liquid fuels. *Chem. Soc. Rev.* **38,** 89–99 (2008).
7. Matthews, H. D. & Solomon, S. Irreversible does not mean unavoidable. *Science* **340,** 438–439 (2013).
8. Gur, I., Sawyer, K. & Prasher, R. Searching for a better thermal battery. *Science* **335,** 1454–1455 (2012).
9. Kucharski, T. J., Tian, Y., Akbulatov, S. & Boulatov, R. Chemical solutions for the closed-cycle storage of solar energy. *Energy Environ. Sci.* **4,** 4449–4472 (2011).
10. Bren', V. A., Dubonosov, A. D., Minkin, V. I. & Chernoivanov, V. A. Norbornadiene–quadricyclane—an effective molecular system for the storage of solar energy. *Russ. Chem. Rev.* **60,** 451–469 (1991).
11. Zen-ichi, Y. New molecular energy storage systems. *J. Photochem.* **29,** 27–40 (1985).
12. Scharf, H-D. *et al.* Criteria for the efficiency, stability, and capacity of abiotic photochemical solar energy storage systems. *Angew. Chem. Int. Ed. Engl.* **18,** 652–662 (1979).
13. Jones G. II, Chiang, S-H. & Xuan, P. T. Energy storage in organic photoisomers. *J. Photochem.* **10,** 1–18 (1979).
14. Dubonosov, A. D., Bren, V. A. & Chernoivanov, V. A. Norbornadiene–quadricyclane as an abiotic system for the storage of solar energy. *Russ. Chem. Rev.* **71,** 917–927 (2002).
15. Boese, R. *et al.* Photochemistry of (fulvalene)tetracarbonyldiruthenium and its derivatives: efficient light energy storage devices. *J. Am. Chem. Soc.* **119,** 6757–6773 (1997).
16. Kanai, Y., Srinivasan, V., Meier, S. K., Vollhardt, K. P. C. & Grossman, J. C. Mechanism of thermal reversal of the (fulvalene)tetracarbonyldiruthenium photoisomerization: toward molecular solar–thermal energy storage. *Angew. Chem. Int. Ed.* **49,** 8926–8929 (2010).
17. Moth-Poulsen, K. *et al.* Molecular solar thermal (MOST) energy storage and release system. *Energy Environ. Sci.* **5,** 8534–8537 (2012).
18. Hou, Z. *et al.* Switching from Ru to Fe: picosecond IR spectroscopic investigation of the potential of the (fulvalene)tetracarbonyldiiron frame for molecular solar-thermal storage. *Phys. Chem. Chem. Phys.* **15,** 7466–7469 (2013).
19. Kolpak, A. M. & Grossman, J. C. Azobenzene-functionalized carbon nanotubes as high-energy density solar thermal fuels. *Nano Lett.* **11,** 3156–3162 (2011).
20. Kolpak, A. M. & Grossman, J. C. Hybrid chromophore/template nanostructures: a customizable platform material for solar energy storage and conversion. *J. Chem. Phys.* **138,** 034303 (2013).
21. Dyke, C. A. & Tour, J. M. Covalent functionalization of single-walled carbon nanotubes for materials applications. *J. Phys. Chem. A* **108,** 11151–11159 (2004).
22. Tasis, D., Tagmatarchis, N., Bianco, A. & Prato, M. Chemistry of carbon nanotubes. *Chem. Rev.* **106,** 1105–1136 (2006).
23. Feng, W., Luo, W. & Feng, Y. Photo-responsive carbon nanomaterials functionalized by azobenzene moieties: structures, properties and application. *Nanoscale* **4,** 6118–6134 (2012).
24. Ying, Y., Saini, R. K., Liang, F., Sadana, A. K. & Billups, W. E. Functionalization of carbon nanotubes by free radicals. *Org. Lett.* **5,** 1471–1473 (2003).
25. Fujino, T., Arzhantsev, S. Y. & Tahara, T. Femtosecond time-resolved fluorescence study of photoisomerization of *trans*-azobenzene. *J. Phys. Chem. A* **105,** 8123–8129 (2001).
26. Han, M. & Hara, M. Intense fluorescence from light-driven self-assembled aggregates of nonionic azobenzene derivative. *J. Am. Chem. Soc.* **127,** 10951–10955 (2005).
27. Han, M. R. & Hara, M. Chain length-dependent photoinduced formation of azobenzene aggregates. *New J. Chem.* **30,** 223–227 (2006).
28. Han, M., Ishikawa, D., Muto, E. & Hara, M. Isomerization and fluorescence characteristics of sterically hindered azobenzene derivatives. *J. Lumin.* **129,** 1163–1168 (2009).
29. Kuhn, H. J., Braslavsky, S. E. & Schmidt, R. Chemical actinometry (IUPAC technical report). *Pure Appl. Chem.* **76,** 2105–2146 (2004).

Acknowledgements
The authors acknowledge financial support from BP for a BP-MIT Postdoctoral Research Associateship (T.J.K.) and research funds awarded through the MIT Energy Initiative, which supported the synthesis of functionalized SWCNTs, and the Advanced Research Projects Agency-Energy (ARPA-E), US Department of Energy, under Award Number DE-AR0000180, which supported all other work. Calculations were performed at the National Energy Research Scientific Computing Center, supported by the Office of Science of the U.S. Department of Energy under Contract No. DE-AC02-05CH11231.

Author contributions
T.J.K. synthesized the materials and performed experiments, N.F. performed solid-state fluorescence and spectroscopy measurements, A.M.K. performed DFT calculations and J.O.Z. performed experiments. All authors contributed to the experimental design, analysed the data and wrote the paper.

Additional information
Supplementary information and chemical compound information are available in the online version of the paper. Reprints and permissions information is available online at www.nature.com/reprints. Correspondence and requests for materials should be addressed to T.J.K., D.G.N. and J.C.G.

Competing financial interests
The authors declare no competing financial interests.